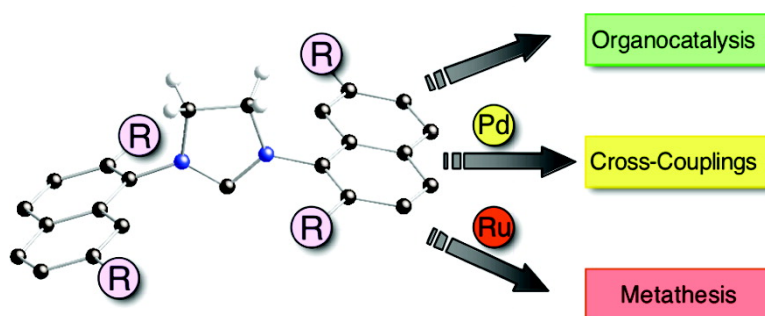


Identification and Characterization of a New Family of Catalytically Highly Active Imidazolin-2-ylidenes

Xinjun Luan, Ronaldo Mariz, Michele Gatti, Chiara Costabile, Albert Poater, Luigi Cavallo, Anthony Linden, and Reto Dorta

J. Am. Chem. Soc., **2008**, 130 (21), 6848-6858 • DOI: 10.1021/ja800861p • Publication Date (Web): 29 April 2008

Downloaded from <http://pubs.acs.org> on February 8, 2009



More About This Article

Additional resources and features associated with this article are available within the HTML version:

- Supporting Information
- Links to the 2 articles that cite this article, as of the time of this article download
- Access to high resolution figures
- Links to articles and content related to this article
- Copyright permission to reproduce figures and/or text from this article

[View the Full Text HTML](#)

Identification and Characterization of a New Family of Catalytically Highly Active Imidazolin-2-ylidenes

Xinjun Luan,[†] Ronaldo Mariz,[†] Michele Gatti, Chiara Costabile,[‡] Albert Poater,[‡] Luigi Cavallo,[‡] Anthony Linden,[†] and Reto Dorta^{*†}

Contribution from the Institute of Organic Chemistry, University of Zurich, Winterthurerstrasse 190, CH-8057, Zurich, Switzerland, and Dipartimento di Chimica, Università di Salerno, Via Ponte don Melillo, Fisciano (SA), I-84084, Italy

Received February 12, 2008; E-mail: dorta@oci.uzh.ch

Abstract: A new class of easily accessible and stable imidazolin-2-ylidenes has been synthesized where the side chains are comprised of substituted naphthyl units. Introduction of the naphthyl groups generates C_2 -symmetric (*rac*) and C_s -symmetric (*meso*) atropisomers, and interconversion between the isomers is studied in detail both experimentally and computationally. Complete characterization of the carbenes includes rare examples of crystallographically characterized saturated NHC structures. Steric properties of the ligands and an investigation of their stability are also presented. In catalysis, the new ligands show versatility comparable to the most widely used NHCs IMes/SIMes or IPr/SIPr. Excellent catalytic results are obtained when either the NHC salts (ring-opening alkylation of epoxides), NHC-modified palladium compounds (C–C and C–N cross-couplings), or NHC–ruthenium complexes (ring-closing metathesis, RCM) are employed. In several cases, this new ligand family provides catalytic systems of higher reactivity than that observed with previously reported NHC compounds.

1. Introduction

The introduction of N-heterocyclic carbenes as ligands for transition metal catalysts and as organic catalysts on their own has put this class of compounds at the forefront of current research efforts.¹ Whereas hundreds of NHCs with various structural motifs have been synthesized and tested in catalysis, bulky, monodentate aryl-substituted imidazol-2-ylidenes (2,4,6-mesityl-substituted IMes and 2,6-isopropylphenyl-substituted IPr) and their saturated imidazolin-2-ylidene counterparts (SIMes and SIPr) still remain the only ligands that represent a truly viable alternative to phosphines, in terms of both versatility and reactivity. Presumably, the perpendicular arrangement of the aryl side chains, combined with the steric bulk on the aromatic rings, leads to a situation where these ligands confer stability to unsaturated and reactive metal centers during catalysis and where decomposition of the catalyst through unwanted metal–ligand interactions is rarely observed. Equally important for their widespread use and success is the simple fact that IMes/SIMes and IPr/SIPr are stable as free carbenes, making them easy to handle and manipulate. In this context, it is of note that

most structures based on saturated imidazolin-2-ylidenes dimerize readily to give enetetramines. This renders saturated NHCs considerably less amenable to catalysis and restricts access to stable modifications of this ligand class. In fact, the tendency of saturated NHCs toward dimerization is so pronounced that very few stable imidazolin-2-ylidenes are known in the literature.^{2,3}

Herein, we describe the synthesis of a series of saturated NHCs that incorporate substituted naphthyl side chains. In order to extend the family of versatile NHC systems for catalysis, we reasoned that 2-substituted naphthyl side chains would be ideally suited for mimicking the successful architectures of the SIMes and SIPr ligand systems (Chart 1). Unexpectedly, the introduction of alkyl substituents on the naphthyl moieties generates atropisomeric ligands with C_2 -symmetric (*rac*) and C_s -symmetric (*meso*) conformations, and we present an in-depth study on the interconversion of these conformers. Whereas the parent naphthyl-substituted NHC ligand proved to be unstable as a free carbene, dimerizing rapidly to form the enetetramine, free carbenes of the other structures were generated in high yield and were characterized by X-ray crystallography.

To test the potential and versatility of our imidazolin-2-ylidenes in catalysis, we selected applications that include palladium and ruthenium catalyzed reactions and an example pertinent to their use in organocatalysis. Throughout, the new

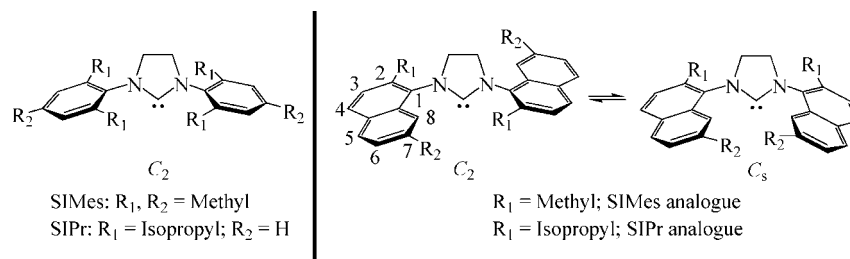
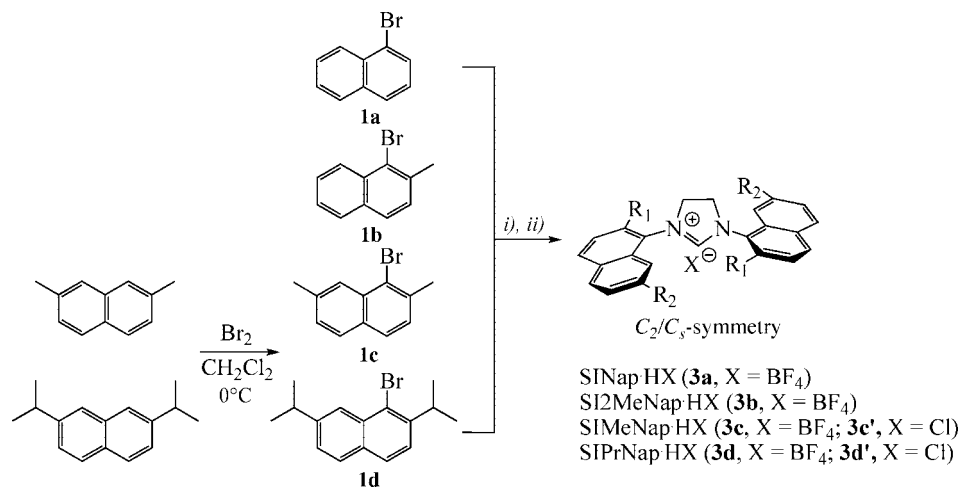
[†] University of Zurich.

[‡] Università di Salerno.

(1) (a) *N-Heterocyclic Carbenes in Synthesis*; Nolan S. P., Ed.; Wiley-VCH: Weinheim, Germany, 2006. (b) *N-Heterocyclic Carbenes in Transition Metal Catalysis*; Glorius, F., Ed.; Topics in Organometallic Chemistry; Springer: Berlin, Germany, 2007; Vol 21. (c) Arduengo, A. J. *Acc. Chem. Res.* **1999**, *32*, 913. (d) Bourissou, D.; Guerret, O.; Gabbai, F. P.; Bertrand, G. *Chem. Rev.* **2000**, *100*, 39. (e) Herrmann, W. A. *Angew. Chem., Int. Ed.* **2002**, *41*, 1290. (f) *Carbene Chemistry. From Fleeting Intermediates to Powerful Reagents*; Bertrand, G., Ed.; Dekker: New York, 2002. (g) Enders, D.; Balensiefer, T. *Acc. Chem. Res.* **2004**, *37*, 534. (h) Peris, E.; Crabtree, R. H. *Coord. Chem. Rev.* **2004**, *248*, 2239. (i) Scott, N. M.; Nolan, S. P. *Eur. J. Inorg. Chem.* **2005**, 1815. (j) Hahn, F. E. *Angew. Chem., Int. Ed.* **2006**, *45*, 1348.

(2) (a) For SIMes and SIPr, see: Arduengo, A. J., III; Goerlich, J. R.; Marshall, W. J. *J. Am. Chem. Soc.* **1995**, *117*, 11027. (b) Arduengo, A. J., III; Krafczyk, R.; Schmundtler, R.; Craig, H. A.; Goerlich, J. R.; Marshall, W. J.; Unverzagt, M. *Tetrahedron* **1999**, *55*, 14523.

(3) (a) For SI^tBu and two derivatives, see: Denk, M. K.; Tadani, A.; Hatano, K.; Lough, A. J. *Angew. Chem., Int. Ed. Engl.* **1997**, *36*, 2607. (b) Denk, M. K.; Hezarkhani, A.; Zheng, F.-L. *Eur. J. Inorg. Chem.* **2007**, 3527.

Chart 1. Imidazolin-2-ylidenes with Phenyl (Left) and Naphthyl (Right) Side Chains**Scheme 1.** Synthesis of Imidazolium Salts^a

^a Reaction conditions: (i) ethylenediamine, $\text{Pd}_2(\text{dba})_3/2(\pm)\text{-BINAP}$ (cat.), NaO^tBu , toluene, 100°C ; (ii) Method A: NH_4BF_4 , HCO_2H (cat.), $\text{HC}(\text{OEt})_3$; Method B: HCl , THF; then $\text{HC}(\text{OEt})_3$, MW.

ligand systems show excellent catalytic activities, and in a number of cases studied, they outperform the existing systems.

2. Results and Discussion

2.1. Synthesis and Characterization of Naphthyl-Based Ligands.

The synthesis of the imidazolium salts **3a–3d** is summarized in Scheme 1. For both 2,7-dimethyl- and 2,7-diisopropynaphthalene, we first devised a bromination protocol to obtain **1c** and **1d**. Bromination in dichloromethane with slight cooling and without addition of any catalyst/initiator provided the best results. Under these optimized reaction conditions, the initial bromination of the naphthyl derivatives turned out to be extremely selective, and after workup, **1c** and **1d** were obtained in quantitative yield. Taking **1a–d**,⁴ and following known synthetic procedures,⁵ gave the saturated NHC salts **3a–3d** in good overall yield and high purity. Elucidation of SINap $\cdot\text{HBF}_4$ [**3a**; 1,3-Bis(naphthalen-1-yl)-imidazolium tetrafluoroborate], SI2MeNap $\cdot\text{HBF}_4$ [**3b**; 1,3-Bis(2-methylnaphthalen-1-yl)-imidazolium tetrafluoroborate], SIMeNap $\cdot\text{HX}$ [**3c** ($X = \text{BF}_4$)/**3c'** ($X = \text{Cl}$); 1,3-Bis(2,7-dimethylnaphthalen-1-yl)-imidazolium salt] and SIPrNap $\cdot\text{HX}$ [**3d** ($X = \text{BF}_4$)/**3d'** ($X = \text{Cl}$); 1,3-Bis(2,7-diisopropynaphthalen-1-yl)-imidazolium salt] by ^1H and ^{13}C NMR spectroscopy showed that SINap $\cdot\text{HBF}_4$ (**3a**) adopts one conformation, while **3b–3d** and **3c'/3d'** gave rise to both *meso* (C_5 -symmetric) and *racemic* (C_2 -symmetric) isomers at room temperature (see discussion below for details). Full characterization of these new imidazolium salts includes

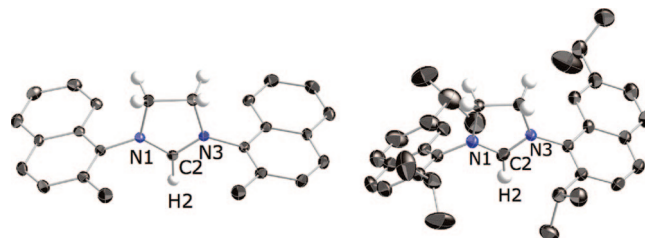


Figure 1. Thermal ellipsoid drawings of imidazolium salts **3b** (left) and **3d'** (right). The anions and the hydrogen atoms except for the backbone and imidazolium protons are omitted for clarity.

single crystal X-ray diffraction studies for **3b** and **3d'**. In both cases, the crystals measured correspond to the C_5 -symmetric (*meso*) species, and thermal ellipsoid drawings of the molecules can be found in Figure 1.

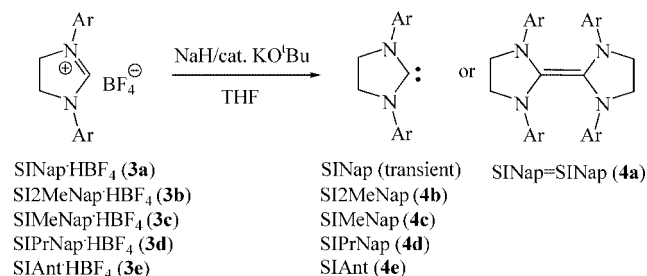
Deprotonation of **3b–3d** with NaH and catalytic amounts of potassium *tert*-butoxide led to clean formation of the free, monomeric carbenes **4b–4d** in high yields (Scheme 2). However, attempts to deprotonate SINap $\cdot\text{HBF}_4$ (**3a**) (or SINap $\cdot\text{HCl}$,⁶) with $\text{NaH}/\text{KO}^t\text{Bu}$, KH/DMSO , or KHMDS invariably led to immediate formation of a bright orange solution containing the dimer SINap $=\text{SINap}$ (**4a**) as the sole observable product.⁷ To test the purely qualitative observation that the instability of **4a** might be due to the lack of the second ortho-substituent found in **4b–4d** (the first one being represented by

(4) Compounds **1a** and **1b** are commercially available.

(5) (a) Scholl, M.; Ding, S.; Lee, C. W.; Grubbs, R. H. *Org. Lett.* **1999**, *1*, 953. (b) Aidouni, A.; Demondeau, A.; Delaude, L. *Synlett* **2006**, 493.

(6) Delaude, L.; Szypa, M.; Demonceau, A.; Noels, A. F. *Adv. Synth. Catal.* **2002**, *344*, 749.

(7) The poor catalytic results reported in ref 6 with “SINap” (generated in situ) are probably due to rapid formation of the dimer.

Scheme 2. Deprotonation of Imidazolium Salts **3a–e**

the fused aromatic ring), we synthesized and fully characterized SIANT·HBF₄ (**3e**, 1,3-Bis(anthracen-9-yl)-imidazolium tetrafluoroborate; see Experimental Section). Indeed, deprotonation of this species, with both ortho positions “protected” by fused aromatic rings, leads to clean formation of monomeric SIANT (**4e**).⁸

According to the ¹H NMR and ¹³C NMR spectra, the deprotonated products **4a–4c** adopt one conformation at 300 K. In the case of dimer **4a**, this implies that only one of the possible regioisomers is formed. For monomers SI2MeNap (**4b**) and SIMeNap (**4c**), the results suggest that deprotonation of the imidazolium salts lead to a situation where the naphthyl side chains are able to freely rotate due to the removal of the NHC–H bond. Finally, examination of the free N-heterocyclic carbene SIPrNap (**4d**) by ¹H NMR and ¹³C NMR spectroscopy at 300 K shows two sets of signals corresponding to the presence of two isomers in an approximately 5:6 ratio (see VT experiments below). Thus, removal of the hydrogen does not seem to alter the initial *rac/meso* ratio, and we can therefore assume that, in this case, a high enough barrier to rotation between the C₂- and C_s-conformations is maintained and no interconversion occurs during deprotonation.

The identities of carbene dimer **4a** and of the free N-heterocyclic carbenes **4c** and **4d** were unambiguously established by single-crystal X-ray crystallography (Figure 2). Crystals of **4a** were obtained by slow evaporation of a saturated THF/Et₂O solution. The solid state structure of **4a** shows a strongly distorted carbene dimer, consistent with the structure of *N,N',N'',N'''*-tetraphenyl-bis(1,3-imidazolidin-2-ylidene).⁹ The side view of the molecule reveals a small tetrahedral distortion at the nitrogen positions and nonplanar five-membered N-heterocycles. Similar distortions in related enetetramines have been documented in the literature and render the nitrogen atoms reactive and accessible, for example, to ready protonation of this type of molecule.¹⁰ Crystals of **4c** suitable for X-ray analysis were obtained by slow evaporation of a saturated Et₂O solution, and crystals of **4d** were grown from saturated pentane/Et₂O solutions. In the solid state, SIMeNap (**4c**) shows its *meso* form, while the measured SIPrNap (**4d**) crystal corresponds to the racemic C₂-symmetric conformer. A comparison of bond lengths and angles with the only two other crystallographically characterized saturated NHCs, namely Arduengo's SIMes^{2a} and

Denk's SI^tBu,^{3a} reveals a similar bonding situation for **4c** and **4d**. The N(1)–C(2)–N(3) angles [104.8(2)°, **4c** and 104.5(2)°, **4d**] are identical to that for SIMes [104.7(3)°] but slightly smaller than that in SI^tBu [106.44(9)°]. A clear difference can be seen in the planarity of the N-heterocycle. Whereas the backbone carbon atoms in SIMes and SI^tBu deviate measurably from the plane of the other three ring atoms, the N-heterocycles in **4c** and **4d** are almost perfectly planar.

2.2. Variable-Temperature ¹H NMR Studies. VT ¹H NMR studies were performed in order to obtain more information on the dynamic behavior of the imidazolium salts and the free imidazolin-2-ylidenes. Figure 3 schematically represents the rotation about the C–N bonds, and color codes show the hydrogen atoms likely to be affected by the rotation.

2.2.1. Imidazolium Salts. VT ¹H NMR spectra of SINap·HBF₄ (**3a**) were measured in acetone-*d*₆ in the temperature range 183–303 K. Only one set of signals was observed for the whole temperature range, meaning that the naphthyl substituents are rotating freely even at low temperature (183 K).

VT ¹H NMR spectra of SI2MeNap·HBF₄ (**3b**) show coalescence of the carbenic proton signals [δ 8.17 (H^{imm}-C₂) and 8.36 (H^{imm}-C_s) ppm] at 370 K (DMSO-*d*₆), and above 380 K the protons of H⁸ (green) and the NHC backbone protons (red) appear as broad singlets, indicating fast interconversion.

VT ¹H NMR studies with different solvents (DMSO-*d*₆ and C₂D₂Cl₄) have been carried out for SIMeNap·HBF₄ (**3c**) and its chloride analogue, SIMeNap·HCl (**3c'**). In this case, the ¹H NMR spectrum of the imidazolium chloride salt **3c'** is identical to that of its corresponding tetrafluoroborate salt **3c** in DMSO-*d*₆. However, significant differences between the spectra of **3c** and **3c'** in C₂D₂Cl₄ at 303 K were observed (Figure 4). The signals of the imidazolium proton in **3c'** shift to a significantly lower magnetic field (ca. 1.0 ppm) with respect to the value for **3c**, presumably reflecting an increased contribution of hydrogen bonding between the H^{imm}-proton and the chloride anion. When raising the temperature to the coalescence temperature, we find that both the nature of the counteranion (BF₄[−] respectively Cl[−]) and the choice of the solvent (DMSO-*d*₆ or C₂D₂Cl₄) do not affect the ease of interconversion for **3c** and **3c'**. Furthermore, the process is almost not affected by the introduction of the 7-methyl group, and coalescence temperatures for SI2MeNap·HBF₄ (**3b**) and SIMeNap·HBF₄ (**3c**) are practically identical.

The VT ¹H NMR spectra in DMSO-*d*₆ of **3d** and **3d'** showed a static behavior, with no detectable line-shape modifications up to 420 K. Undoubtedly, the decrease in fluxional behavior is caused by the increased size of the ortho-substituents on the naphthyl moieties (isopropyl vs methyl).

2.2.2. Free NHCs. VT ¹H NMR experiments were also performed on solutions of **4b–4d**. In the case of **4b** and **4c**, interconversion of the two atropisomeric conformations at room temperature leads to the observation of a single signal for the H⁸ protons (δ = 8.18 ppm for **4b** and δ = 8.02 ppm for **4c** in toluene-*d*₈). Lowering the temperature showed gradual broadening of these signals with decoalescence at 273 K (**4b**) and 293 K (**4c**). The formation of two sets of ¹H NMR signals in the slow-exchange regime is again consistent with the dynamic interconversion between *meso*- and *rac*-conformers. With SIPrNap (**4d**), two sets of signals were observed at room temperature and fully attributed to the *rac* and *meso* forms. By raising the temperature, coalescence of the resonance signals at δ 8.00 and 8.10 ppm (H⁸ proton) was achieved at 350 K,

(8) In order to obtain stable, saturated NHCs with aromatic side chains, structures where both ortho-hydrogens are substituted seem to be ideal. Preliminary studies on NHCs with phenyl side chains and only one ortho-substitution (methyl, isopropyl) produce rather unstable monomers.

(9) Hitchcock, P. B. *J. Chem. Soc., Dalton Trans.* **1979**, 1314.

(10) (a) Hitchcock, P. B.; Lappert, M. F.; Pye, P. L. *J. Chem. Soc., Dalton Trans.* **1977**, 2160. (b) Duijn, M. A.; Lutz, M.; Spek, A. L.; Elsevier, C. J. *J. Organomet. Chem.* **2005**, *690*, 5804.

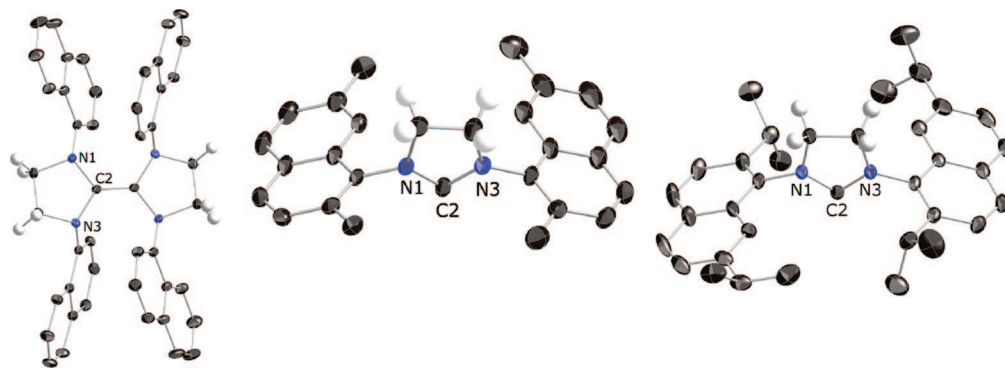


Figure 2. Thermal ellipsoid views of the SINap=SiNap (**4a**, left), *meso*-SiMeNap (**4c**, middle) and *rac*-SiPrNap (**4d**, right). Hydrogen atoms on the side chains are omitted for clarity.

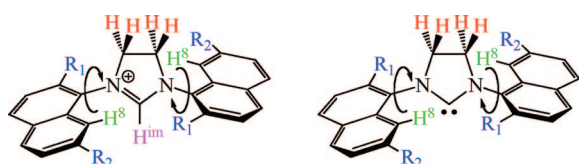


Figure 3. Schematic representation of the interconversion between the atropisomers.

and above 360 K the signal appeared as a sharp singlet at δ 8.02 ppm (Figure 5).

2.2.3. Activation Free Energies. From the VT analyses performed above, we calculated activation free energies ΔG^\ddagger at the coalescence temperature (T_c) for the interconversion, using complete line-shape analysis,¹¹ which gave the corresponding ΔG^\ddagger (kJ mol⁻¹) values (Table 1). It is evident from the data that the rotational barriers decrease in the order (**3d = 3d'**) > (**3c = 3c'**) \approx **3b** > **3a** for the salts and **4d** > **4c** > **4b** for the free NHCs. These trends can be clearly associated with the steric demand of the naphthyl side chains. More specifically, substituents at both the 2- and 7-positions of the naphthyl moieties affect ΔG^\ddagger , with the 2-position playing a crucial factor limiting the rotation about the C–N bond between the side chains and the five-membered central ring. Moreover, ΔG^\ddagger decreases by about 20 kJ mol⁻¹ when removing the carbenic proton, that is when going from the imidazolium salts to the free carbenes.

2.3. Calculations on the Chemical/Conformational Stability and Steric Characterization of the Ligands. DFT calculations in the solvent phase confirm that the *rac* and *meso* isomers of **4b–d** are of substantially the same energy (within 3 kJ mol⁻¹), and this difference is scarcely dependent on the solvent, since calculations in THF or toluene resulted in very similar values (within 1–2 kJ mol⁻¹). In excellent agreement with the experimental ΔG^\ddagger 's, the DFT barrier in toluene for the interconversion of the *rac* isomer into the *meso* isomer is quite similar in **4b** and **4c** (around 54 kJ mol⁻¹) and increases to 70 kJ mol⁻¹ in **4d**. Rotation in the monomeric species SINap, instead, presents the negligible barrier of 3 kJ mol⁻¹. With regards to the dimerization of the free NHCs to the corresponding enetetramines, we calculated that dimerization of SINap in THF is favored by 15 kJ mol⁻¹, whereas **4b–d** were calculated to be thermodynamically stable as monomers. However, while **4b** and **4c** are slightly more stable than the dimer (by 10 and

29 kJ mol⁻¹, respectively), dimerization of **4d** is remarkably unfavored (by 106 kJ mol⁻¹). Similar excellent agreement between the DFT and the experimental values is obtained for the rotational barriers in the **3a–3d** salts. In all cases, the salts present a barrier to rotation roughly 20 kJ mol⁻¹ higher than that in the corresponding free NHC.

These results clearly support the idea that the behavior of SINap and **4b–4d** is determined by the nature of the group in position 2 of the binaphthyl framework. With a hydrogen atom in this position, such as in SINap, rotation around the N–naphthyl bond is completely free, and dimerization to the enetetramine SINap=SiNap (**4a**) is favored. With a methyl group in this position, such as in **4b** and **4c**, rotation around the N–naphthyl bond presents a moderate barrier, and dimerization is moderately disfavored. Finally, with a bulky isopropyl group in this position, such as in **4d**, rotation around the N–Ar bond is frozen at room temperature, and dimerization is clearly unfavored.

To further characterize this new ligand family, we calculated the percent of buried volume % V_{Bur} , a molecular descriptor that can be considered as an analogue of Tolman's cone angle for tertiary phosphines,¹² and that can be successfully used to classify the steric properties of NHC ligands.^{13,14} Table 2 shows that the % V_{Bur} of SINap is smaller than the value previously calculated for SIMes (% V_{Bur} = 27), while % V_{Bur} of **4b** and **4c** indicate a slightly bulkier nature than their mesityl-substituted counterparts. It is of interest to note that the % V_{Bur} of the *meso* isomer is usually smaller than that of the *rac* isomer. Finally, the % V_{Bur} of SiPrNap (**4d**) is somewhat larger than the % V_{Bur} of the SiPr ligand (% V_{Bur} = 30). In short, this analysis confirms the starting hypothesis that **4b** and **4c** should substantially mimic the IMes/SIMes ligands, while the steric requirements of **4d** are best compared to the SiPr ligand.

2.4. Catalytic Applications: Palladium Catalysis. Pioneering work by Nolan et al. has shown that NHC-modified Pd-allyl catalysts are extremely active systems in various cross-coupling reaction protocols.¹⁵ By following their experimental procedure, addition of [Pd(allyl)Cl]₂ to free carbenes **4b–d** gave high yields of *rac/meso* mixtures of our compounds with general formula

(11) Friebolin, H. *Basic One- and Two-Dimensional NMR Spectroscopy*; VCH: New York, 1991; Chapter 11.

(12) Tolman, C. A. *Chem. Rev.* **1977**, *77*, 313.

(13) Cavallo, L.; Correa, A.; Costabile, C.; Jacobsen, H. *J. Organomet. Chem.* **2005**, *690*, 5407.

(14) Hillier, A. C.; Sommer, W. J.; Yong, B. S.; Peterson, J. L.; Cavallo, L.; Nolan, S. P. *Organometallics* **2003**, *22*, 4322.

(15) (a) Viciu, M. S.; Navarro, O.; Germaneau, R. F.; Navarro-Fernandez, O.; Stevens, E. D.; Nolan, S. P. *Organometallics* **2002**, *21*, 5470. (b) Viciu, M. S.; Germaneau, R. F.; Nolan, S. P. *Org. Lett.* **2002**, *4*, 4053. (c) Navarro, O.; Kaur, H.; Mahjoor, P.; Nolan, S. P. *J. Org. Chem.* **2004**, *69*, 3173.

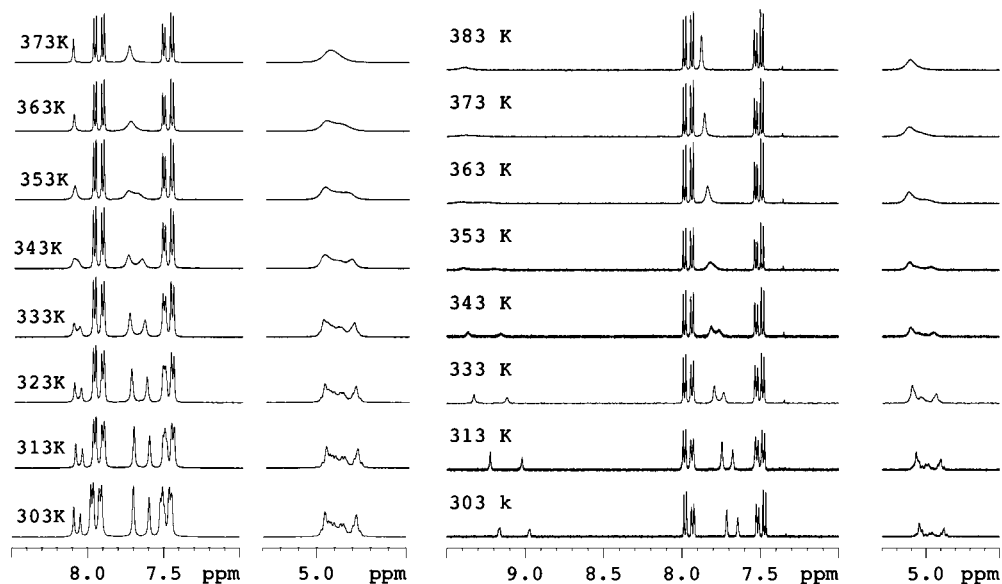


Figure 4. VT ^1H NMR spectra (500 MHz) of SIMeNap·HBF $_4$ (**3c**, left) and SIMeNap·HCl (**3c'**, right) in $\text{C}_2\text{D}_2\text{Cl}_4$.

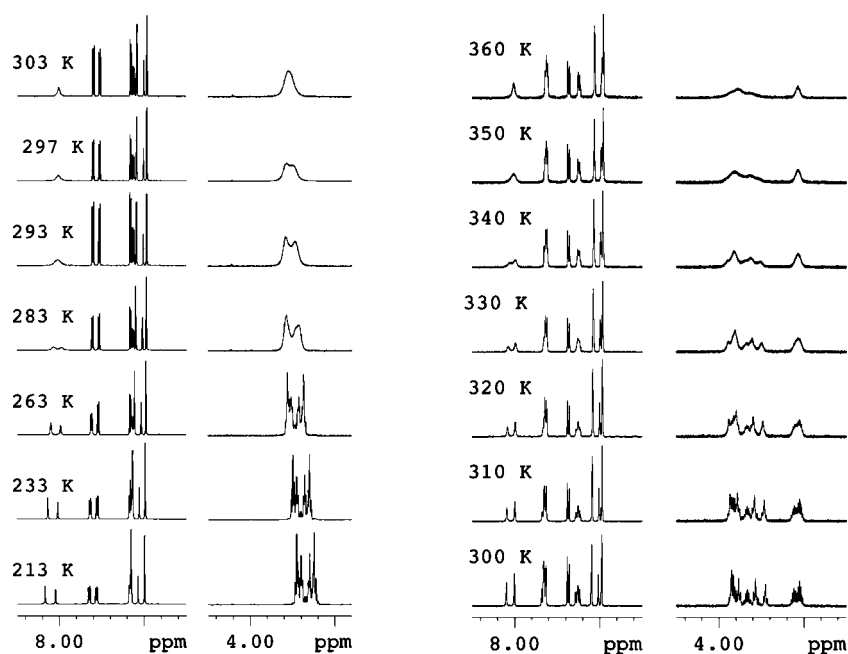


Figure 5. VT ^1H NMR spectra (400 MHz) of free carbenes **4c** (left) and **4d** (right) in toluene- d_8 .

Table 1. Values of T_c , the Corresponding ΔG^\ddagger 's and DFT Values for ΔG^\ddagger

entry	compound	solvent	T_c (K)	ΔG^\ddagger (kJ mol $^{-1}$)	DFT ΔG^\ddagger (kJ mol $^{-1}$)
1	3a	acetone- d_6	<183	<44.1	30
2	3b	DMSO- d_6	370 (H^8)	74.6	75
3	3c	$\text{C}_2\text{D}_2\text{Cl}_4$	353 (H^{im})	75.5	74
4	3c'	$\text{C}_2\text{D}_2\text{Cl}_4$	373 (H^{im})	75.5	-
5	3c or 3c'	DMSO- d_6	350 (H^{im})	75.6	-
6	3d or 3d'	DMSO- d_6	>410	>89.9	80
7	4b	toluene- d_8	273 (H^8)	56.9	54
8	4c	toluene- d_8	293 (H^8)	59.8	54
9	4d	toluene- d_8	350 (H^8)	74.4	70

Table 2. Steric Parameter % V_{Bur} Corresponding to SINap and **4b–4d**

entry	NHC	% V_{Bur}	
		<i>rac</i> -isomer	<i>meso</i> -isomer
1	SINap	26	26
2	SI2MeNap (4b)	28	27
3	SIMeNap (4c)	29	28
4	SIPrNap (4d)	31	31
5	IMes		26 ^a
6	SIMes		27 ^a
7	IPr		29 ^a
8	SIPr		30 ^a

^a Values taken from ref 13.

(NHC)Pd(allyl)Cl (**5b–d**). Attempts to separate these *rac/meso* mixtures via column chromatography using a variety of different eluents were unsuccessful, and the compound mixtures were

recovered unchanged. In contrast, repeated crystallization from CH_2Cl_2 /hexane and ethyl acetate/hexane (see Experimental

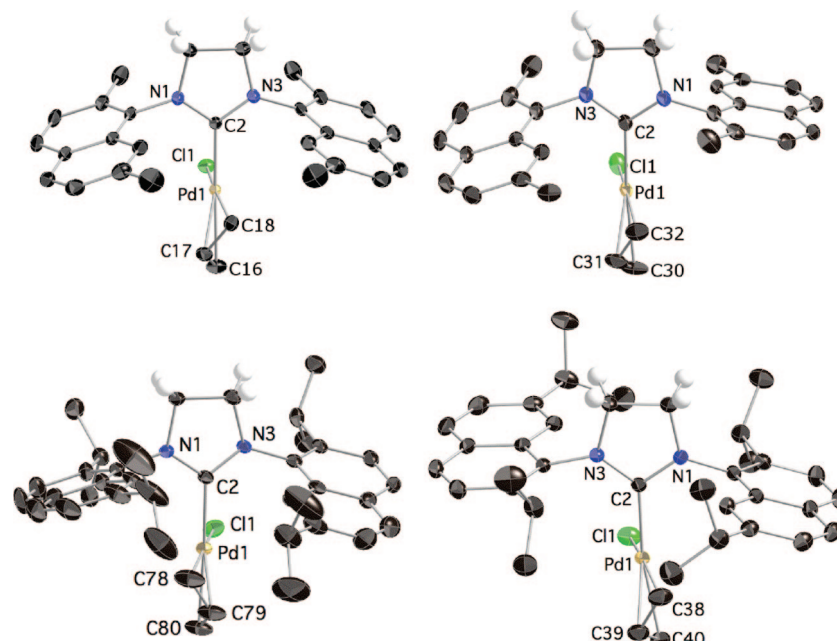


Figure 6. Crystal structures of (*meso*-SiMeNap)Pd(allyl)Cl (*meso*-**5c**, top left), *rac*-SiMeNapPd(allyl)Cl (*rac*-**5c**, top right), (*meso*-SiPrNap)Pd(allyl)Cl (*meso*-**5d**, bottom left), and *rac*-SiPrNapPd(allyl)Cl (*rac*-**5d**, bottom right).

Section) enabled the separation of both **5c** and **5d** into *meso*-**5c**, *rac*-**5c** and *meso*-**5d**, *rac*-**5d**, respectively. NMR analyses gave distinct signals for the *rac* and *meso* complexes, and to assign their conformation unambiguously, the crystal structures of all four compounds were determined (Figure 6). As could be anticipated from the studies on our NHC salts, the formation of the NHC–metal bond efficiently freezes the rotation around the C–N bonds of the NHC side chains.

Considering the excellent performance of DFT in reproducing the experimental rotational barrier between the *rac* and *meso* isomers in the free NHCs, we used the same approach to predict the *rac* to *meso* rotational barrier in the catalytically active compounds, presumed to have the formula (NHC)Pd(0). Even for the less encumbered (Si2MeNap)Pd(0) and (SiMeNap)Pd(0) intermediates, we found a high barrier for rotation (102 and 103 kJ mol⁻¹ in toluene), which suggests that the respective symmetry of the ligands (*rac* or *meso*) should be retained during catalysis.

Initial catalytic studies with our palladium complexes indicated that the reactivity of *meso*-**5c** (*meso*-**5d**) is essentially the same as the reactivity seen for *rac*-**5c** (*rac*-**5d**) (see Supporting Information). For convenience, all of the following catalytic applications were therefore run with *rac*/*meso* mixtures of the precatalysts. Rather bulky substrates were chosen in the Suzuki–Miyaura cross-coupling reactions of aryl chlorides (Table 3, entries 1–20). Especially when both coupling partners are ortho-substituted (entries 1–10), our naphthyl-based catalysts perform better than the corresponding (SiMes)Pd(allyl)Cl [**SiMes-Nolan**] and (SiPr)Pd(allyl)Cl [**SiPr-Nolan**] systems and display high activity at 80 °C.¹⁶ Significant reactivity differences among **5b**–**5d** can only be seen when the reactions are run at room temperature, where SiPrNap-modified **5d** gives better conversions than the catalysts derived from methyl-substituted **5b** and

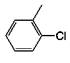
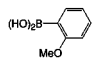
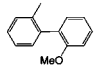
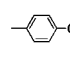
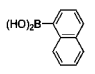
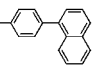
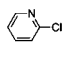
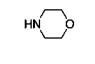
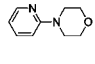
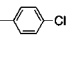
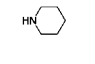
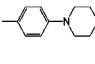
5c. In contrast, activity differences are dramatic in the Hartwig–Buchwald amination with difficult aryl-chloride substrates (entries 21–31), where we see an enormous drop in catalyst performance when moving from the SiPr/SiPrNap systems (excellent reactivity) to SiMes-, Si2MeNap-, and SiMeNap-modified palladium complexes, which are rather poor catalysts for the substrates studied. In these amination protocols, small changes in the sterics of the NHC ligand system seem to have a big impact on the activity of the catalysts and the bulkiest systems (**SiPr-Nolan** and **5d**) become the catalysts of choice for these transformations.

2.5. Ruthenium Catalysis. One of the most important applications of NHCs in metal catalysis is undoubtedly their use as ligands in Ru-catalyzed metathesis reactions.¹⁷ The general interest in these transformations compelled us to examine analogues of Grubbs' second generation catalyst [RuCl₂(SiMes)(=CHPh)(PCy₃)],^{17c} incorporating ligand systems **4b**–**d**. Synthesis was achieved by simple exchange of one phosphine ligand with NHCs **4b**–**d** in toluene.^{17b} Appropriate workup gave [RuCl₂(Si2MeNap)(=CHPh)(PCy₃)] (**6b**), [RuCl₂(SiMeNap)(=CHPh)(PCy₃)] (**6c**), and [RuCl₂(SiPrNap)(=CHPh)(PCy₃)] (**6d**) in good yields. We then employed catalysts **6b**–**6d** in the ring-closing metathesis (RCM) of three standard substrates (Table 4, entries 1–14). Except for a slightly lower reaction temperature (27 °C instead of 30 °C), standard reaction conditions were used,¹⁸ and the conversions were monitored by ¹H NMR spectroscopy. While the reactivities of **6b** and **6c** closely resemble that seen with SiMes-modified Grubbs II, catalyst **6d** gave markedly superior results. In fact, **6d** outperforms Grubbs II by an order of magnitude, and the RCM of all three substrates runs to completion in less than 1 h with only

(16) For “Second-generation” catalysts with modified allyl moieties showing vastly superior reactivity, see: Marion, N.; Navarro, O.; Mei, J.; Stevens, E. D.; Scott, N. M.; Nolan, S. P. *J. Am. Chem. Soc.* **2006**, *128*, 4101.

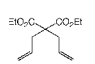
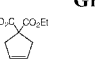
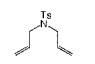
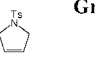
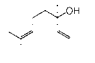
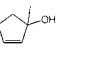
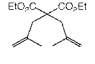
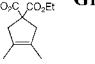
(17) (a) For first reports, see Weskamp, T.; Schattenmann, W. C.; Spiegler, M. M.; Herrmann, W. A. *Angew. Chem., Int. Ed.* **1998**, *37*, 2490. (b) Huang, J.; Stevens, E. D.; Nolan, S. P.; Peterson, J. L. *J. Am. Chem. Soc.* **1999**, *121*, 2674. (c) Scholl, M.; Ding, S.; Lee, C. W.; Grubbs, R. H. *Org. Lett.* **1999**, *1*, 953.
(18) Ritter, T.; Hejl, A.; Wenzel, A. G.; Funk, T. W.; Grubbs, R. H. *Organometallics* **2006**, *25*, 5740.

Table 3. Selected Pd-Catalyzed C–C and C–N Couplings with **5b–d**

Entry	Ar-Cl	Amine or B-acid	Product ^[c]	Catalyst (1 mol%)	Time	Temp.	Yield ^[a]
1				SIMes-Nolan	1h	80°C	<5%
2				5b	1h	80°C	98%
3				5c	1h	80°C	98%
4				SIPr-Nolan	1h	80°C	59%
5				5d	1h	80°C	99%
6				SIMes-Nolan	16h	RT	<5%
7				5b	16h	RT	43%
8				5c	16h	RT	58%
9				SIPr-Nolan	16h	RT	57%
10				5d	16h	RT	75%
11				SIMes-Nolan	1h	80°C	82%
12				5b	1h	80°C	95%
13				5c	1h	80°C	97%
14				SIPr-Nolan	15min	80°C	86%
15				5d	15min	80°C	99%
16				SIMes-Nolan	16h	RT	79%
17				5b	16h	RT	75%
18				5c	16h	RT	81%
19				SIPr-Nolan	3h	RT	83%
20				5d	3h	RT	98%
21				SIMes-Nolan	24h	RT	88%
22				5b	24h	RT	95%
23				5c	96h	RT	89%
24				SIPr-Nolan	1min	RT	99%
25				5d	1min	RT	99%
26				5d (0.1 mol%)	6h	RT	95%
27				SIMes-Nolan	20h	80°C	11%
28				5b	20h	80°C	23%
29				5c	20h	80°C	4%
30				SIPr-Nolan	10min	80°C	99%
31				5d	10min	80°C	99%

^a Yields determined by GC against internal standard. Reaction times and conditions of the reference systems (SIMes)Pd(allyl)Cl [**SIMes-Nolan**] and (SIPr)Pd(allyl)Cl [**SIPr-Nolan**] were chosen according to the results for **5b/5c** and **5d**, respectively.

Table 4. RCM of Standard Dienes Employing Catalysts **6b–d**

Entry	Diene	Product	Catalyst	Loading (mol%)	Temp.	t (min)	Conv. ^[a]
1			Grubbs II	1	30°C	42	98% ^[b]
2			6b	1	27°C	70	98%
3			6c	1	27°C	65	98%
4			6d	1	27°C	17	98%
5			6d	0.1	27°C	52	98%
6			Grubbs II	1	25°C	90	98% ^[c]
7			6b	1	27°C	54	98%
8			6c	1	27°C	28	98%
9			6d	1	27°C	10	100%
10			6d	0.1	27°C	25	100%
11			6b	1	27°C	18	100%
12			6c	1	27°C	19	100%
13			6d	1	27°C	7	100%
14			6d	0.1	27°C	35	100%
15			Grubbs II	5	30°C	96 h	17% ^[b]
16			6b	5	27°C	72 h	30%
17			6c	5	27°C	72 h	40%
18			6d	5	27°C	72 h	31%

^a Conversions determined by ¹H NMR spectroscopy. For better comparison, a fixed conversion of 98% was used for entries 1–8.^b Taken from ref 18.^c Taken from ref 21a.

0.1 mol% of **6d**, corresponding to turnover frequencies for complete conversion at 27 °C of up to 2400 TOF (entry 10). Even trisubstituted diolefin linalool reacts readily under these conditions, at the same time showing a pronounced induction period that is absent for the other two substrates or at 1 mol% catalyst loading (Figure 7). Interestingly, the introduction of alkylated naphthyl side chains renders catalysts **6b–d** more active toward the RCM of diethyltrimethylsilyl malonate (entries 15–18).¹⁹ In recent years, enhancement of reactivities by fine-tuning [RuCl₂(SIMes)(=CHPh)(PCy₃)] (Grubbs II) have been

observed and have by and large been achieved by modifying every other entity of the precatalyst.^{20–23} Unfortunately, such approaches often involve additional synthetic steps and are normally exclusive and limited to ruthenium metathesis. On the other hand, successful modifications to the NHC structure as presented here with SIPrNap may prove valuable in a plethora of other catalytic applications and certainly highlight the pivotal role played by the NHC ligand architecture in these systems.²⁴

2.6. Alkylation of Epoxides. With the excellent catalytic results obtained above in both palladium and ruthenium mediated reactions, we finally wanted to see whether our systems could

- (19) (a) For recent examples by Grubbs et al. showing higher conversions, see: Berlin, M. J.; Campbell, K.; Ritter, T.; Funk, T. W.; Chlenov, A.; Grubbs, R. H. *Org. Lett.* **2007**, *9*, 1339. (b) Stewart, I. C.; Ung, T.; Pletnev, A. A.; Berlin, J. M.; Grubbs, R. H.; Schrodri, Y. *Org. Lett.* **2007**, *9*, 1589.
- (20) (a) For Hoveyda–Grubbs catalyst, see: Garber, S. B.; Kingsbury, J. S.; Gray, B. L.; Hoveyda, A. H. *J. Am. Chem. Soc.* **2000**, *122*, 8168.
- (21) (a) For modifications of the Hoveyda–Grubbs catalyst, see: Wakamatsu, H.; Blechert, S. *Angew. Chem., Int. Ed.* **2002**, *41*, 794. (b) Wakamatsu, H.; Blechert, S. *Angew. Chem., Int. Ed.* **2002**, *41*, 2403. (c) Grela, K.; Harutyunyan, S.; Michrowska, A. *Angew. Chem., Int. Ed.* **2002**, *41*, 4038. (d) Michrowska, A.; Bujok, R.; Harutyunyan, S.; Sashuk, V.; Dolgonos, G.; Grela, K. *J. Am. Chem. Soc.* **2004**, *126*, 9318.
- (22) (a) For modifications of Grubbs II, see: Conrad, J. C.; Amoroso, D.; Czechura, P.; Yap, G. P. A.; Fogg, D. E. *Organometallics* **2003**, *22*, 3634. (b) Love, J. A.; Sanford, M. S.; Day, M. W.; Grubbs, R. H. *J. Am. Chem. Soc.* **2003**, *125*, 10103. (d) Conrad, J. C.; Parnas, H. H.; Snelgrove, J. L.; Fogg, D. E. *J. Am. Chem. Soc.* **2005**, *127*, 11882.
- (23) For a very elegant modification of Grubbs II, see: Romero, P. E.; Piers, W. E.; McDonald, R. *Angew. Chem., Int. Ed.* **2004**, *43*, 6161.
- (24) For recent examples pertinent to NHC modification of Grubbs II, see ref 19 and: Ritter, T.; Day, M. W.; Grubbs, R. H. *J. Am. Chem. Soc.* **2006**, *128*, 11768.

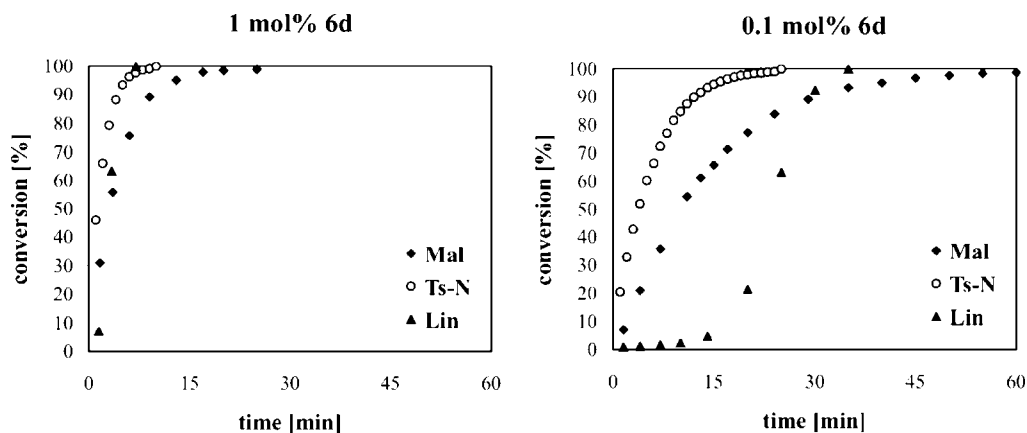
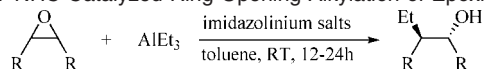


Figure 7. Conversion to product at 27 °C with 1 mol% (left) and 0.1 mol% (right) of catalyst **6d**. Abbreviations used: Mal (Diethyldiallyl malonate), Ts-N (*N,N*-Diallyl-4-methyl-benzenesulfonamide), and Lin (Linalool).

Table 5. NHC-Catalyzed Ring-Opening Alkylation of Epoxides



Entry	Epoxide	Product	Catalyst	Loading (mol%)	t (h)	Yield ^[a]
1			AsPh ₃	5	24	94% ^[b]
2			SIPr·HBF ₄	5	12	71% ^[c]
3			DMSIPr·HBF ₄	5	12	93% ^[c]
4			3b	1	12	98%
5			3c	1	12	95%
6			3d	1	12	93%
7			AsPh ₃	5	24	75% ^{[b],[d]}
8			DMSIPr·HBF ₄	5	12	77% ^[c]
9			3b	1	24	90%
10			3c	1	24	91%
11			3d	1	24	97%
12			AsPh ₃	5	24	62% ^[b]
13			DMSIPr·HBF ₄	5	12	53% ^[c]
14			3b	1	20	61%
15			3c	1	20	78%
16			3d	1	20	96%

^a Yields after workup, determined by GC against internal standard.

^b Taken from ref 25. ^c Taken from ref 26. ^d Reaction conducted at 50 °C.

also be used as catalytic Lewis bases for the ring-opening alkylation of epoxides by alkylaluminum reagents. Initial studies by Schneider et al. on the use of phosphine and arsine bases in these transformations²⁵ have more recently been followed by Nguyen's finding that bulky NHC salts could also be employed.²⁶ The best NHC-derived catalyst turned out to be a substructure of SIPr·HBF₄ with two additional methyl groups on the backbone of the N-heterocycle (for simplicity, we call this ligand DMSIPr·HBF₄), whereas Schneider et al. have identified AsPh₃ as the best base in their studies. The reactivities of SI2MeNap·HBF₄ (**3b**), SIMeNap·HBF₄ (**3c**), and SIPrNap·HBF₄ (**3d**) are superior to those of the benchmark catalysts reported in the literature (Table 5). In fact, catalytic ring-opening of cyclohexene oxide could be easily run with only 1 mol% of catalyst (versus 5 mol% for the reference systems) and resulted in products of equal or higher yields (entries 1–6). Even better results were obtained with more challenging substrates cyclopentene oxide and 2,3-butene oxide (entries 7–16). Furthermore, buildup of side products as observed by Nguyen et al. with SIPr·HBF₄ and DMSIPr·HBF₄ was not observed with our

catalysts. Within our ligand family, we again identify the isopropyl-substituted SIPrNap·HBF₄ (**3d**) as the most competent substructure, giving almost quantitative yields with all products.

3. Conclusions

We have presented a new class of saturated NHC ligands with naphthyl-derived side chains. An initial, highly selective bromination protocol was devised for some of the substituted naphthyl moieties and renders the synthetic pathway to all of the imidazolium salts easy and straightforward. Deprotonation of the salts yielded a dimer in the case of SINap, whereas, with substituted naphthyl as well as with anthracenyl side chains, high yields of the free carbenes and rare examples of crystallographically characterized imidazolin-2-ylidenes were obtained. The stability of the monomers is explained by using computational methods. In both the NHC salts and the free carbenes, introduction of substituted naphthyl side chains gives rise to *C*₂-symmetric (*rac*) and *C*_s-symmetric (*meso*) atropisomers. In-depth experimental and computational analyses for the inter-conversion between the two isomers showed that as soon as the NHC carbon atom is bound to either a hydrogen (for the NHC salt) or a metal (NHC-Pd), the rotation around the C–N bonds becomes highly unfavorable.

At the outset of the present study, we sought the identification of viable N-heterocyclic carbene alternatives to the widely used and versatile IMes/SIMes and IPr/SIPr architectures. The preliminary catalytic results presented here exceeded our expectations. We were not only able to demonstrate that this new naphthyl-based NHC ligand family presents similar versatility to the reference systems and can (at least) be employed in palladium-based coupling reactions, in ruthenium-based metathesis, and in the organocatalytic ring-opening alkylation of epoxide but also, more importantly, show that catalytic activities were at least as high or higher than those in the reference systems. In the palladium-catalyzed reactions, generally better reactivities than those with the corresponding SIMes- and SIPr-modified Nolan catalysts were obtained, with SIPrNap outperforming the methyl-substituted ligands. Better still, the naphthyl-substituted NHCs described here are the catalysts of choice for the organocatalytic ring-opening alkylation of epoxides, giving higher yields of products at lower catalyst loadings than the reference systems described in the literature. Of possibly even greater significance is the identification of precatalyst [RuCl₂(SIPrNap)(=CHPh)(PCy₃)] (**6d**) as a rapidly initiating species in metathesis. In fact, the preliminary results

(25) (a) Schneider, C.; Brauner, J. *Tetrahedron Lett.* **2000**, *41*, 3043. (b) Schneider, C.; Brauner, J. *Eur. J. Org. Chem.* **2001**, 4445.

(26) Zhou, H.; Campbell, J.; Nguyen, S. T. *Org. Lett.* **2001**, *3*, 2229.

here show that **6d** outperforms Grubbs II in the ring-closing metathesis by an order of magnitude, making it a very appealing alternative to existing catalyst systems.

One of our long-term goals is the identification of a family of broadly applicable chiral NHC ligands, and we believe that the unique architecture of the naphthyl-based N-heterocyclic carbenes we describe here presents an ideal starting point for such a study.

4. Experimental Section

4.1. General Information. All reactions were carried out under a nitrogen atmosphere using standard Schlenk lines or gloveboxes (Mecaplex or Innovative Technology). All reagents were used as received unless otherwise noted. Solvents were purchased in the best quality available, degassed by purging thoroughly with nitrogen and dried over activated molecular sieves of appropriate size. Alternatively, they were purged with argon and passed through alumina columns in a solvent purification system (Innovative Technology). Solvents for NMR spectroscopy were degassed with nitrogen and dried over molecular sieves. NMR spectra were recorded on AV2 400 or AV2 500 MHz Bruker spectrometers. Multiplicities are abbreviated as follows: singlet (s), doublet (d), triplet (t), quartet (q), doublet-doublet (dd), quintet (quint), septet (sept), multiplet (m), and broad (br). High-resolution mass spectra (HRMS) were performed on a Finnigan MAT 95 (Finnigan MAT95, San Jose, CA; USA) double-focusing magnetic sector mass spectrometer (geometry BE). ESI mass spectra were performed on a triple stage quadrupole instrument (Finnigan TSQ 700, San Jose, CA; USA), equipped with a combined Finnigan Atmospheric Pressure Ion (API) source. GC-MS analysis was done on a Finnigan Voyager GC8000 Top. GC analyses of reaction mixtures were carried out on a Trace GC 2000 equipped with an FID detector. The column used was a 30-m ZB-5 capillary column with 0.25-mm inner diameter and 0.25- μ m film thickness. Flow rate = 1.5 mL/min for He carrier gas. GC yields were determined through integration of the product peak against internal standard using pre-established response factors. Retention times for various components of the reaction mixture were assigned by injection of a pure sample of each component. X-ray crystallography was performed on a Nonius Kappa CCD area-detector diffractometer using graphite-monochromated Mo K α radiation ($\lambda = 0.71073$ Å) and an Oxford Cryosystems Cryostream 700 cooler. *N,N*-Diallyl-4-methylbenzenesulfonamide was prepared according to a literature procedure.²⁷

4.2. Allylchloro[1,3-bis(2-methylnaphthalen-1-yl)-imidazolin-2-ylidene]palladium [(S)MeNap]Pd(allyl)Cl (5b). **4b** (280 mg, 0.80 mmol) and [Pd(allyl)Cl]₂ (146 mg, 0.40 mmol) were mixed together in a vial in the glovebox. Dry THF (20 mL) was added, and the mixture was stirred at room temperature for 12 h. The solvent was decanted, and the solid was washed with 5 mL of cold THF and dried *in vacuo*. The crude product was dissolved in 10 mL of CH₂Cl₂ and filtered through a celite filter to remove traces of palladium black. The white powder **5b** was obtained as a 1:1 mixture of the two atropisomers bearing *meso*- and *rac*-**4b**, respectively (325 mg, 76%). ¹H NMR (CDCl₃, 400 MHz): δ 8.05–7.76 (m, 6H), 7.66–7.58 (m, 2H), 7.50–7.40 (m, 4H), 4.34–4.17 (m, 4H), 4.48–4.45 (m, 0.2H), 4.08–3.96 (m, 0.8H), (corresponding to the atropisomers of one proton), 3.53 (d, $J = 7.5$ Hz, 0.2H), 3.45 (d, $J = 7.5$, 0.8H), (corresponding to the atropisomers of one proton), 3.03 (d, $J = 6.6$ Hz, 0.5H), 2.88 (d, $J = 6.6$ Hz, 0.5H), (corresponding to the atropisomers of one proton), 2.88 (s, 1.5H), 2.76 (s, 3H), 2.74 (s, 1.5H), (corresponding to the atropisomers of six protons), 2.37–2.27 (m, 1H), 1.62 (d, $J = 12.2$ Hz, 0.2H), 1.10 (d, $J = 12.2$ Hz, 0.8H) (corresponding to the atropisomers of one proton). ¹³C NMR (CDCl₃, 100 MHz) (due to the existence of the atropisomers, the ¹³C NMR spectrum is

complex): 214.45, 214.34, 213.99, 136.32, 136.08, 134.80 (two signals overlapped), 134.53, 134.36, 134.25, 133.38, 133.31, 133.25, 131.07, 131.01, 130.89, 129.98, 129.92, 129.14, 129.09, 128.92, 128.87, 128.79, 128.74, 128.33 (two signals overlapped), 127.06, 126.98, 126.91, 126.58, 125.90 (two signals overlapped), 125.52, 125.39, 123.54 (two signals overlapped), 122.30, 122.21, 114.77, 114, 66, 72.25, 72.17, 72.06, 52.42, 52.29, 52.25, 51.11, 50.51, 49.78, 19.54, 19.22, 19.15. HRMS (ESI) m/z calculated for C₂₈H₂₇PdN₂ [M – Cl]⁺ 495.1210, observed 495.1211.

4.3. Allylchloro[1,3-bis(2,7-dimethylnaphthalen-1-yl)-imidazolin-2-ylidene]palladium [(S)MeNap]Pd(allyl)Cl (5c). **4c** (930 mg, 2.46 mmol) and [Pd(allyl)Cl]₂ (449 mg, 1.23 mmol) were mixed together in a vial in the glovebox. Dry THF (20 mL) was added, and the mixture was stirred at room temperature for 1.5 h. The solvent was removed *in vacuo*, and 20 mL of hexane were added to triturate the product. The reaction mixture was filtered in air, and the solid washed with hexane. The two isomers were successfully separated by repeated fractional crystallization with CH₂Cl₂/hexane to yield 662 mg of **5c_{meso}** (48% yield) and 400 mg of **5c_{rac}** (23% yield). Crystals suitable for diffraction studies were grown from CH₂Cl₂/hexane solutions.

Data for **5c_{meso}** are as follows. ¹H NMR (CDCl₃, 400 MHz): δ 7.78–7.70 (m, 6H), 7.40 (d, $J = 8.4$ Hz, 1H), 7.34 (d, $J = 8.4$ Hz, 1H), 7.32–7.29 (m, 2H), 4.29–4.24 (m, 4H), 4.05–3.95 (m, 1H), 3.45 (dd, $J = 7.5$, 2.5 Hz, 1H), 2.87–2.85 (m, 1H), 2.81 (s, 3H), 2.72 (s, 3H), 2.59 (s, 6H), 2.29 (d, $J = 12.2$ Hz, 1H), 1.11 (d, $J = 12.2$ Hz, 1H). ¹³C NMR (CDCl₃, 100 MHz): 214.27, 136.34, 136.30, 136.14, 136.01, 133.95, 133.68, 131.58, 131.17, 131.05, 129.11, 129.09, 129.08, 129.06, 128.77, 128.49, 128.43, 127.63, 127.49, 121.57, 121.42, 114.66, 71.89, 52.17, 52.11, 50.79, 22.62, 19.51, 19.49. HRMS (ESI) m/z calculated for C₃₀H₃₁PdN₂ [M – Cl]⁺ 523.1523, observed 523.1528.

Data for **5c_{rac}** are as follows. ¹H NMR (CDCl₃, 400 MHz): δ 7.79–7.70 (m, 6H), 7.36–7.33 (m, 2H), 7.30–7.26 (m, 2H), 4.35–4.31 (m, 0.4H), 4.23 (s, 4H), 4.14–4.04 (m, 0.6H), 3.51 (dd, $J = 7.5$, 2.5 Hz, 0.4H), 3.44 (dd, $J = 7.5$, 2.5 Hz, 0.6H), 3.09 (dd, $J = 6.6$, 2.0 Hz, 0.6H), 3.05 (dd, $J = 6.6$, 2.0 Hz, 0.4H), 2.79 (s, 1.2H), 2.78 (s, 1.8H), 2.59 (s, 1.8H), 2.57 (s, 1.2H), 2.29–2.26 (m, 1H), 1.57, (d, $J = 1.8$ Hz, 0.6H), 1.26 (d, $J = 1.8$ Hz, 0.4H). ¹³C NMR (CDCl₃, 100 MHz) (due to existence of two isomers, ¹³C NMR spectrum appeared complex): 214.58, 214.16, 136.67, 136.66, 134.32, 134.31, 134.09, 131.69, 131.66, 131.21, 131.19, 128.63, 128.58, 128.09, 128.04, 122.98, 122.90, 114.64, 72.17, 72.02, 52.41, 49.87, 49.33, 22.50, 19.08, 18.99. HRMS (ESI) m/z calculated for C₃₀H₃₁PdN₂ [M – Cl]⁺ 523.1523, observed 523.1528.

4.4. Allylchloro[1,3-bis(2,7-diisopropyl-naphthalen-1-yl)-imidazolin-2-ylidene]palladium [(S)PrNap]Pd(allyl)Cl (5d). **4d** (1020 mg, 2.07 mmol) and [Pd(allyl)Cl]₂ (377 mg, 1.03 mmol) were mixed together in a round-bottom flask in the glovebox. Dry THF (50 mL) was added, and the mixture was stirred at room temperature for 1.5 h. The solvent was removed *in vacuo*, and 30 mL of hexane were added to triturate the product. The reaction mixture was filtered in air, and the solid was washed with hexane. The two isomers were successfully separated by fractional crystallization with EtOAc/hexane to yield 585 mg of **5d_{meso}** (42% yield) and 544 mg of **5d_{rac}** (36% yield).

Data for **5d_{meso}** are as follows. ¹H NMR (CDCl₃, 400 MHz): δ 7.86–7.73 (m, 6H), 7.53 (d, $J = 8.7$ Hz, 1H), 7.49 (d, $J = 8.7$ Hz, 1H), 7.45–7.38 (m, 2H), 4.35–4.20 (m, 4H), 4.16–4.08 (m, 1H), 3.83, (sept, $J = 6.8$ Hz, 1H), 3.68, (sept, $J = 6.8$ Hz, 1H), 3.48 (dd, $J = 7.5$, 2.0 Hz, 1H), 3.21–3.13 (m, 2H), 2.87–2.85 (m, 1H), 2.35 (d, $J = 13.4$ Hz, 1H), 1.61–1.22 (m, 24H), 1.10 (d, $J = 12.1$ Hz, 1H). ¹³C NMR (CDCl₃, 100 MHz): 213.97, 147.38, 146.87, 146.22, 145.70, 133.09, 132.78, 132.02, 131.87, 130.89, 130.30, 129.15, 129.14, 129.12, 124.47, 124.45, 124.33, 123.89, 120.38, 120.05, 114.48, 71.56, 60.60, 53.92, 53.59, 51.08, 35.90, 35.70, 31.80, 29.01, 28.90, 26.04, 26.01, 24.93, 24.83, 24.15, 24.11, 24.03,

(27) Varray, S.; Lazaro, R.; Martinez, J.; Lamaty, F. *Organometallics* **2003**, *22*, 2426.

24.01, 23.67, 22.87, 21.26, 14.42, 14.32. HRMS (ESI) m/z calculated for $C_{30}H_{31}PdN_2ClNa$ $[M + Na]^+$ 693.2361, observed 693.2373.

Data for **5d_{rac}** are as follows. 1H NMR ($CDCl_3$, 500 MHz): δ 7.86–7.75 (m, 6H), 7.47–7.38 (m, 4H), 4.64–4.59 (m, 0.8H), 4.35–4.29 (m, 4H), 4.08–4.01 (m, 0.2H), 3.90–3.82 (m, 2H), 3.60 (dd, $J = 7.5, 2.4$ Hz, 0.8H), 3.51 (dd, $J = 7.5, 2.4$ Hz, 0.2H), 3.16 (sept, $J = 6.8, 2H$), 2.95–2.93 (m, 0.8H), 2.79–2.77 (m, 0.2H), 2.48–2.42 (m, 1H), 1.78 (d, $J = 11.9$ Hz, 0.2H), 1.50–1.36 (m, 24H), 0.78 (d, $J = 11.9$ Hz, 0.8H). ^{13}C NMR ($CDCl_3$, 100 MHz) (due to existence of two isomers, ^{13}C NMR spectrum appeared complex): 214.38, 213.27, 147.12, 147.06, 144.69, 144.51, 133.17, 133.10, 131.93, 131.83, 131.02, 130.99, 129.25, 129.22, 128.29, 128.21, 126.40, 126.21, 123.51, 123.47, 120.43, 120.35, 114.62, 114.58, 72.58, 52.27, 53.69, 53.63, 50.24, 49.69, 34.65, 34.61, 28.88, 28.82, 25.91, 25.63, 24.10, 23.94, 23.87, 23.71, 23.66, 23.54. HRMS (ESI) m/z calculated for $C_{30}H_{31}PdN_2ClNa$ $[M + Na]^+$ 693.2361, observed 693.2373.

4.5. {RuCl₂[1,3-bis(2-methylnaphthalen-1-yl)-imidazolin-2-ylidene](=CH–Ph)(PCy₃)} [RuCl₂(SI2MeNap)(=CHPh)(PCy₃)] (6b**).** **4b** (300 mg, 0.85 mmol) and $RuCl_2(=C(H)Ph)(PCy_3)_2$ (700 mg, 0.85 mmol) were mixed together in a 200 mL flask in the glovebox. Dry toluene (40 mL) was added, and the mixture was stirred at room temperature for 16 h. The solvent was removed *in vacuo*, washed with 4×10 mL of hexane, and then dissolved in minimum CH_2Cl_2 and precipitated with Et_2O /pentane (1:3). Filtration of the pink precipitate afforded the product **6b** in 65% (495 mg) yield. 1H NMR (CD_2Cl_2 , 400 MHz, 273 K) exists as a mixture of atropisomers: δ 19.04 (s, $Ru=CHPh$), 19.01 (s, $Ru=CHPh$), 18.48 (s, $Ru=CHPh$), 18.45 (s, $Ru=CHPh$), (corresponding to the atropisomers of one proton), 8.87–6.09 (m, ArH , 17H), 4.31–3.93 (m, NCH_2CH_2N , 4H), 3.44–2.33 (m, $ArCH_3$, 6H), 1.93–0.40 (m, PCy_3 , 33H). ^{13}C NMR (CD_2Cl_2 , 100 MHz, 300 K) (due to the existence of the atropisomers, the ^{13}C NMR spectrum is complex): δ 294.92, 222.61, 221.85, 151.19, 138.15, 137.78, 136.46, 135.80, 134.37, 133.89, 133.36, 133.33, 132.04, 131.88, 131.36, 131.18, 130.22, 130.20, 129.94, 129.38, 129.20, 129.12, 128.18, 128.12, 128.04, 127.95, 127.25, 127.09, 126.92, 126.50, 126.21, 126.19, 125.69, 124.77, 121.51, 31.98, 31.96, 31.81, 31.79, 29.41, 29.23, 28.27, 28.23, 28.16, 28.06, 26.65, 21.16, 21.04, 19.49, 19.31. ^{31}P NMR (CD_2Cl_2 , 162 MHz, 273 K): δ 30.96, 30.48, 29.92. HRMS (ESI) m/z calculated for $C_{50}H_{60}PRuN_2$ $[M - 2Cl - H]^+$ 815.3571, observed 815.3556.

4.6. {RuCl₂[1,3-bis(2,7-dimethyl-naphthalen-1-yl)-imidazolin-2-ylidene](=CH–Ph)(PCy₃)} [RuCl₂(SIMeNap)(=CHPh)(PCy₃)] (6c**).** **4c** (322 mg, 0.85 mmol) and $RuCl_2(=C(H)Ph)(PCy_3)_2$ (700 mg, 0.85 mmol) were mixed together in a 200 mL flask in the glovebox. Dry toluene (40 mL) was added, and the mixture was stirred at room temperature for 16 h. The solvent was removed *in vacuo*, washed with 4×10 mL of hexane, and then dissolved in minimum CH_2Cl_2 and precipitated with Et_2O /pentane (1:3). Filtration of the pink precipitate afforded the product **6c** in 73% (575 mg) yield. 1H NMR (CD_2Cl_2 , 400 MHz, 260 K) exists as a mixture of atropisomers: δ 18.97 (s, $Ru=CHPh$), 18.94 (s, $Ru=CHPh$), 18.44 (s, $Ru=CHPh$), 18.40 (s, $Ru=CHPh$), (corresponding to the atropisomers of one proton), 9.09–6.08 (m, ArH , 15H), 4.25–3.88 (m, NCH_2CH_2N , 4H), 3.05–2.22 (m, $ArCH_3$, 12H), 1.92–0.36 (m, PCy_3 , 33H). ^{13}C NMR (CD_2Cl_2 , 100 MHz, 273 K) (due to the existence of the atropisomers, the ^{13}C NMR spectrum is complex): δ 295.99, 294.61, 293.95, 293.51, 223.50, 222.74, 221.87, 221.52, 221.11, 160.66, 160.45, 151.32, 150.56, 150.45, 139.75, 139.56, 137.37, 136.82, 136.58, 136.18, 135.90, 135.78, 135.63, 135.34, 135.06, 134.81, 134.52, 133.57, 133.36, 132.19, 131.84, 131.61, 131.50, 131.24, 130.68, 130.03, 129.75, 129.61, 129.35, 129.28, 129.15, 129.09, 128.81, 128.61, 128.21, 128.09, 127.76, 127.56, 126.87, 126.29, 126.21, 124.43, 123.87, 123.27, 122.90, 119.86, 34.55, 32.05, 31.53, 31.39, 31.24, 29.25, 29.12, 28.83, 28.55, 25.05, 27.96, 27.87, 26.44, 23.13, 22.83, 22.57, 22.43, 22.25, 20.82, 19.31, 19.06, 18.91, 14.41, 14.35. ^{31}P NMR (CD_2Cl_2 , 162 MHz, 270 K):

δ 30.45, 29.48, 29.09. HRMS (ESI) m/z calculated for $C_{52}H_{64}PRuN_2$ $[M - 2Cl - H]^+$ 843.3883, observed 843.3878.

4.7. {RuCl₂[1,3-bis(2,7-diisopropyl-naphthalen-1-yl)-imidazolin-2-ylidene](=CH–Ph)(PCy₃)} [RuCl₂(SIPrNap)(=CHPh)(PCy₃)] (6d**).** **4d** (170 mg, 0.347 mmol) and $RuCl_2(=C(H)Ph)(PCy_3)_2$ (277 mg, 0.336 mmol) were mixed together in a vial in the glovebox. Dry toluene (19 mL) was added, and the mixture was stirred at room temperature for 28 h. After transferring it into a flask, the solvent was removed *in vacuo*. The content was dissolved in diethyl ether and filtered over cotton (6 mL total). Then, methanol was layered on top of it (14 mL), and the vial was put into the freezer for 6 h. The precipitate was taken out of the freezer and left at room temperature for an additional hour. Then, the mother liquor was decanted off and precipitation was repeated once more (4 mL diethylether/15 mL methanol). Decantation was followed by drying *in vacuo*. From the combined mother liquors, another crop of pure pink product was obtained. Combined yield: 81% (280 mg). 1H NMR (CD_2Cl_2 , 400 MHz, 300 K) exists as a mixture of atropisomers: δ 19.23 (s, $Ru=CHPh$), 19.20 (s, $Ru=CHPh$), (corresponding to the atropisomers of one proton), 8.56–6.66 (m, ArH , 15H), 4.42–3.14 (m, $NCH_2CH_2N + ArCH(CH_3)_2$, 8H), 1.98–0.56 (m, $ArCH_3 + PCy_3$, 57H). ^{13}C NMR (CD_2Cl_2 , 100 MHz, 300 K) (due to the existence of the atropisomers, the ^{13}C NMR spectrum is complex): δ 294.58, 293.28, 222.82, 222.05, 150.77, 150.64, 147.58, 147.21, 146.66, 146.48, 145.23, 144.98, 135.28, 135.10, 133.14, 132.99, 132.57, 131.96, 131.83, 131.76, 131.53, 131.25, 131.21, 130.48, 130.42, 129.54, 129.50, 128.15, 128.10, 127.88, 127.62, 126.61, 125.89, 125.58, 124.96, 124.17, 124.12, 124.07, 123.21, 123.16, 122.39, 120.85, 54.72, 51.00, 35.53, 35.45, 35.07, 34.80, 32.10, 32.01, 31.94, 31.84, 29.86, 29.74, 29.30, 29.24, 29.02, 28.57, 28.53, 28.26, 28.16, 28.07, 26.70, 26.46, 25.93, 25.83, 24.65, 24.58, 24.54, 24.17, 24.05, 23.39, 23.23, 23.14, 22.86. ^{31}P NMR (CD_2Cl_2 , 162 MHz, 300 K): δ 29.49, 29.22. HRMS (ESI) m/z calculated for $C_{60}H_{80}PRuN_2$ $[M - 2Cl - H]^+$ 961.5107.

4.8. Suzuki–Miyaura Cross-Coupling Reactions: General Procedure. In a glovebox, to a vial closed with a screw cap fitted with a septum and equipped with a magnetic stir bar were added in turn catalyst (1 mol %), potassium *tert*-butoxide (124 mg, 1.1 mmol), boronic acid (1.05 mmol), 2-propanol (1 mL), and dodecane (216 μ L, 1 mmol). The mixture was then stirred at room temperature. After 15 min, the aryl chloride (1 mmol) was injected. If the reaction was carried out at 80 °C, the aryl chloride was injected outside the glovebox. The reaction was monitored by gas chromatography, and the yields were determined through integration of the product against dodecane (internal standard) using pre-established response factors.

2'-Methyl-2-methoxybiphenyl (Table 3, entries 1–10):²⁸ $t_R = 11.84$ min (80 °C, 3 min, 15 °C/min).

1-(4-Methylphenyl)naphthalene (Table 3, entries 11–20):²⁹ $t_R = 14.79$ min (80 °C, 3 min, 15 °C/min).

4.9. Hartwig–Buchwald Cross-Coupling Reactions. General Procedure. In a glovebox, to a vial closed with a screw cap fitted with a septum and equipped with a magnetic stir bar were added in turn catalyst (1 mol %), potassium *tert*-butoxide (124 mg, 1.1 mmol), anhydrous DME (1 mL), and dodecane (216 μ L, 1 mmol). The mixture was then stirred at room temperature. After 5 min, the aryl chloride (1 mmol) and the amine (1.1 mmol) were injected. If the reaction was carried out at 80 °C, the aryl chloride and the amine were injected outside the glovebox. The reaction was monitored by gas chromatography, and the yields were determined through integration of the product against dodecane (internal standard) using pre-established response factors.

4.10. Hartwig–Buchwald Cross-Coupling Reactions at Low Catalyst Loading. In a glovebox, 0.01 mmol of complex (**6.7 mg** of **5d**) was dissolved in 10 mL of DME, providing catalyst solution

(28) Kataoka, N.; Shelby, Q.; Stambuli, J. P.; Hartwig, J. F. *J. Org. Chem.* **2002**, *67*, 5553.

(29) Nishimura, M.; Ueda, M.; Miyaura, N. *Tetrahedron* **2002**, *58*, 5779.

A. To another vial closed with a screw cap fitted with a septum and equipped with a magnetic stir bar were added in turn potassium *tert*-butoxide (124 mg, 1.1 mmol), catalyst solution A (1 mL, 0.1 mol %), and dodecane (216 μ L, 1 mmol). The mixture was then stirred at room temperature. After 5 min, the aryl chloride (1 mmol) and the amine (1.1 mmol) were injected. The reaction was monitored by gas chromatography, and the yields were determined through integration of the product against dodecane (internal standard) using pre-established response factors.

***N*-(2-Pyridyl)morpholine** (Table 3, entries 21–26):³⁰ $t_R = 10.05$ min (80 °C, 3 min, 15 °C/min).

***N*-(4-Methylphenyl)piperidine** (Table 3, entries 27–31):³¹ $t_R = 11.31$ min (80 °C, 3 min, 15 °C/min).

4.11. RCM of Diethyldiallyl Malonate in the Presence of 1 mol% of Catalyst. An NMR tube with a screw cap sample top was charged inside the glovebox with 0.80 mL of CD₂Cl₂ catalyst solution 0.0010 M (0.80 μ mol, 1.0 mol%). The sample was equilibrated at 300 K in the NMR instrument before the substrate (19.3 μ L, 19.2 mg, 0.080 mmol) was added via syringe. Data points were collected after an appropriate period of time. The conversion was determined by comparing the ratio of the integrals of methylene protons in the starting material, δ 2.61 (dt), with those in the product, δ 2.98 (s).

4.12. RCM of Diethyldiallyl Malonate in the Presence of 0.1 mol% of Catalyst. An NMR tube with a screw cap sample top was charged inside the glovebox with 0.080 mL of CD₂Cl₂ catalyst solution 0.0010 M (0.080 μ mol, 0.1 mol%) and 0.72 mL of CD₂Cl₂. The sample was equilibrated at 300 K in the NMR instrument before the substrate (19.3 μ L, 19.2 mg, 0.080 mmol) was added via syringe.

4.13. RCM of Linalool in the Presence of 1 mol% of Catalyst. An NMR tube with a screw cap sample top was charged inside the glovebox with 0.80 mL of CD₂Cl₂ catalyst stock solution 0.0010 M (0.80 μ mol, 1.0 mol%). The sample was equilibrated at 300 K in the NMR instrument before the substrate (14.3 μ L, 12.3 mg, 0.080 mmol) was added via syringe. Data points were collected after an appropriate period of time. The conversion was determined by comparing the ratio of the integrals of methyl protons in the starting material, δ 1.24 (s), with those in the product, δ 1.34 (s).

4.14. RCM of Linalool in the Presence of 0.1 mol% of Catalyst. An NMR tube with a screw cap sample top was charged inside the glovebox with 0.080 mL of CD₂Cl₂ catalyst stock solution 0.0010 M (0.080 μ mol, 0.1 mol%) and 0.72 mL of CD₂Cl₂. The sample was equilibrated at 300 K in the NMR instrument before the substrate (14.3 μ L, 12.3 mg, 0.080 mmol) was added via syringe.

4.15. RCM of *N,N*-Diallyl-4-methyl-benzenesulfonamide in the Presence of 1 mol% of Catalyst. An NMR tube with a screw cap sample top was charged inside the glovebox with 0.40 mL of a CD₂Cl₂ catalyst stock solution 0.0020 M (0.80 μ mol). The sample was equilibrated at 300 K in the NMR instrument before 0.4 mL of a CD₂Cl₂ solution of the substrate (18.9 mg, 0.080 mmol) was added via syringe. Data points were collected after an appropriate period of time. The conversion was determined by comparing the ratio of the integrals of methylene protons in the starting material, δ 3.77 (d), with those in the product, δ 4.08 (s).

4.16. RCM of *N,N*-Diallyl-4-methyl-benzenesulfonamide in the Presence of 0.1 mol% of Catalyst. An NMR tube with a screw cap sample top was charged inside the glovebox with 0.76 mL of a CD₂Cl₂ solution of the substrate (18.9 mg, 0.080 mmol). The sample was equilibrated at 300 K in the NMR instrument before 0.040 mL of a CD₂Cl₂ catalyst stock solution 0.0020 M (0.080 μ mol) was added via syringe.

4.17. RCM of Diethyl-2,2-di(2-methylallyl)malonate in the Presence of 5 mol% of Catalyst. An NMR tube with a screw cap sample top was charged inside the glovebox with 0.40 mL of CD₂Cl₂ catalyst solution 0.010 M (0.004 mmol, 5.0 mol%) and 0.40 mL of CD₂Cl₂ solution of the substrate (21.5 mg, 0.08 mmol). The sample was kept at 300 K for 72 h. The conversion was determined by comparing the ratio of the integrals of methylene protons in the starting material, δ 2.71 (s), with those in the product, δ 2.90 (s).

4.18. General Reaction Procedure for the Alkylation of Meso Epoxides. All reactions were carried out in a glovebox, and the epoxides were dried over CaH₂ and stored inside a glovebox. Into a 20 mL vial equipped with a magnetic stir bar were added the epoxide (1.0 mmol), internal standard (30 mg, 0.22 mmol), and toluene (2 mL). Subsequently, the catalyst (1 mol %) and the triethylaluminum reagent (1.1 mL, 2.0 mmol) were added, and the reaction was stirred at room temperature for 12–24 h.

The reaction was quenched with HCl (4 mL of a 1 M solution in H₂O) and extracted with ether (3 \times 5 mL). The combined organic extracts were washed successively with brine (10 mL) and H₂O (10 mL) and dried over MgSO₄. The solution was filtered, and an aliquot was analyzed by GC to determine the yield.

***trans*-2-Ethyl-1-cyclohexanol** (Table 5, entries 4–6):³² $t_R = 6.49$ min (80 °C, 10 °C/min).

***trans*-2-Ethyl-1-cyclopentanol** (Table 5, entries 7–11):³³ $t_R = 4.71$ min (80 °C, 3 min, 10 °C/min).

***anti*-2-Hydroxy-3-methylpentane** (Table 5, entries 12–16):³⁴ $t_R = 8.08$ min (40 °C, 6 min, 10 °C/min).

Acknowledgment. R.D. holds an Alfred Werner Assistant Professorship and thanks the foundation for generous financial support. X.L. thanks the University of Zurich for support through a Drittmittelkredit. We thank Prof. Jay S. Siegel and LPF (Labor für Prozessforschung, OCI) for a generous donation of 2,7-dimethylnaphthalene. L.C. thanks the INSTM (Cineca Grant) for financial support. A.P. thanks the MEC for a postdoctoral grant.

Note Added after ASAP Publication. Table 3 contained alignment errors in the version published on the Web April 29, 2008. The correct version posted May 2, 2008 and the print version are correct.

Supporting Information Available: Experimental procedures for the ligands, spectroscopic data, computational methods, and crystallographic data (CIF). This material is available free of charge via the Internet at <http://pubs.acs.org>.

JA800861P

(30) Wagaw, S.; Buchwald, S. L. *J. Org. Chem.* **1996**, *61*, 7240.

(31) Barluenga, J.; Aznar, F.; Fernandez, M. *Chem.—Eur. J.* **1997**, *3*, 1629.

(32) Jones, J. B.; Takemura, T. *Can. J. Chem.* **1982**, *60*, 2950.

(33) (a) Brown, H. C.; Jadhav, P. K.; Mandal, A. K. *J. Org. Chem.* **1982**, *47*, 5074. (b) Cannone, P.; Bernatchez, M. *J. Org. Chem.* **1987**, *52*, 4025.

(34) Berrada, S.; Desert, S.; Metzner, P. *Tetrahedron* **1988**, *44*, 3575.